Pure & Appl. Chem., Vol. 67, No. 1, pp. 209–216, 1995.
Printed in Great Britain.

Photochemistry in LB films and its application to molecular switching devices

I. Yamazaki and N. Ohta

Department of Chemical Engineering, Faculty of Engineering, Hokkaido University, Sapporo 060, Japan

Abstract: Molecular orientation and aggregation of functional guest molecules in LB monolayer films were studied by means of the polarized absorption and the Stark effect measurements. A method of controlling the molecular dispersion is presented. As an example of *sequential* and *cooperative* photochemical processes in LB multilayer films, we demonstrate a sequential excitation energy transport and its optical switching by using a photochromic LB film, and discuss its applicability to an optically switching molecular device.

INTRODUCTION

Recent advance in molecular photophysics is directed toward supramolecular systems in which functional chromophores are linked together, and also toward molecular assemblies, e.g., lipid bilayers, LB films, polymers and liquid crystals which are characterized by the structural orders intermediate between crystal and liquid. Photoexcited molecules under restricted geometries might show dynamical behaviors different from homogeneous systems of solution, glass or crystal (1). It must play a fundamental role in the photophysical processes of biological systems in which different kinds of functional molecules are located in polypeptide chains with the specific order, and a cooperative and sequential reaction takes place inside a network of somewhat weak but quite effective molecular interactions (2).

We have studied photochemical processes in LB mono- and multi-layer films as an artificial analog of the biological molecular networks. Fundamental knowledge on structures and photochemical behaviors in LB films has been obtained, and it has been applied to an optical molecular switching device. The present paper will review our study on LB films: (1) *Structure and its control of LB films*, (2) *Photochemical processes in LB films* and (3) *Application to an optically switching molecular device.*

STRUCTURE AND ITS CONTROL OF LB FILMS

Molecular Orientation of Functional Guest Molecules

The LB film is a mono- or multi-layered molecular assembly which is prepared by transferring a compressed monolayer spread on a water surface onto a substrate (3). One can prepare the LB film containing photochemically reactive chromophores with their number densities being variable over a wide range. The molecular orientation in LB monolayer films was investigated with the polarized absorption measurement for cyanine dyes and aromatic hydrocarbons (4). In an optical arrangement shown in Fig. 1, the absorbance is measured as functions of the polarization angle of incident light (β) and the rotation angle of the LB film

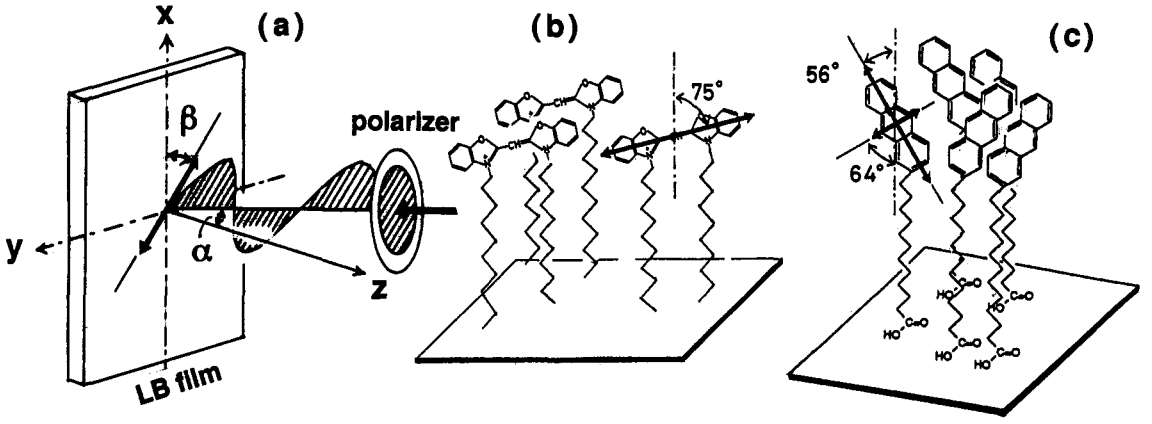

Fig. 1. (a) Optical arrangement in the polarized absorption measurement for LB films; α, the angle between the incident light and the z axis of the film; β, the angle between the direction of light polarization and the x axis of the film. (b) and (c) Molecular orientation of oxacyanine and anthracene in LB films.

rotating around the vertical axis (α). From the experimental curves and the known direction of the transition dipole moment(s) for $S_0 \rightarrow S_1$ and/or $S_0 \rightarrow S_2$, the angles of molecular orientation in the LB film were determined. Figure 1 shows two examples of the LB films of oxacyanine (30 mol% in a mixture of arachidic acid and methylarachidate, 1:1) and anthracene (30 mol% in stearic acid). In the LB film generally, the angles of molecular orientation take particular values (average) characteristic of molecule.

Fractal Structures in Molecular Dispersion of Guest Molecules

Spatial dispersion of functional guest molecules in LB films takes quite irregular and nonuniform structures, so-called "island" structure (5). In most cases, the distribution pattern can be analyzed in terms of a fractal or fractal-like structure: The fractal dimension is $\bar{d}$=1.3-1.5 for cationic dyes such as rhodamine B and cyanines (6,7,9), and $\bar{d}$=1.7-2.0 for neutral aromatic hydrocarbons (8). Excited molecules undergo in a primary step an energy migration among fractal-like distributed sites and energy trapping at higher aggregates.

Molecular Aggregation: Stark Effect on Absorption spectra

In relation to the "island" structure of molecular dispersion and the compression of guest molecules within a cage of fatty acid matrix, guest molecules form specific aggregates in the LB film; the ground-state dimers and higher aggregates (J-aggregates)(3) and the excited-state dimers (excimers) have been studied for cyanine dyes and aromatic hydrocarbons (11), i.e, naphthalene, fluorene (8), anthracene, phenanthrene and perylene. As an example, oxacyanine (see Fig. 1b) forms aggregates depending on concentration (7). Figure 2 shows the absorption spectra and plots of the maximum wavelength of absorption and fluorescence bands at concentration of 0.015-30 mol%. At a concentration of less than 0.2 mol%, monomers as dominant sites are photoexcited, and emit the monomer fluorescence, while at higher concentration, the mixture of monomer and dimer is photoexcited, and the dimer fluorescence is emitted.

Recently we studied influence of electric fields on absorption (so-called electrochromism) of cyanine dyes in LB monolayer films by an electromodulation technique (10). Based on the analysis of the Stark shift, the direction and the magnitude of change in the electric dipole ($\Delta\mu$) and in the polarizability ($\Delta\alpha$) associated with excitation into S_1 has been determined at different concentrations of oxacyanine. The change in absorbance by an external electric field (F_Z) can be regarded as a perturbation, and the absorbance at excitation energy E, $A(E, F_Z)$, is given by

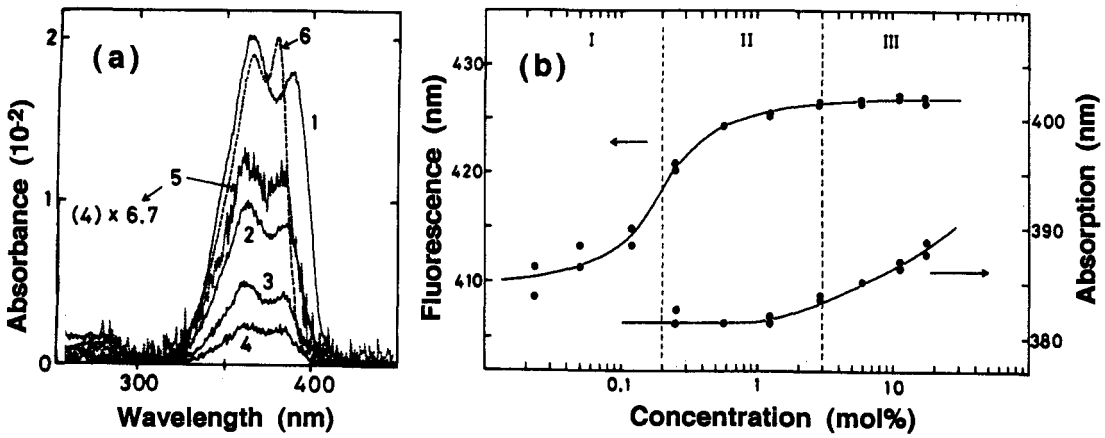

Fig. 2. (a) Absorption spectra of oxacyanine LB films and (b) plots of maximum wavelengths in the absorption and fluorescence bands *versus* concentration of oxacyanine.

$$A(E, F_Z) = A(E, 0) - (dA/dE)\Delta\mu_Z F_Z + (1/2)\,[(d^2A/dE^2)(\Delta\mu_Z F_Z)^2 - (dA/dE)\,\Delta\alpha\, F_Z^2] \qquad (1)$$

When the change in transmittance is very small, the absorbance change can be written by using the transmited light intensity, $I(E)$, as;

$$A(E, F_Z) - A(E, 0) = -\,[\Delta I(E) / I(E)] / 2.303, \qquad \text{where } \Delta I(E) = I(E, F_Z) - I(E, 0) \qquad (2)$$

Figure 3 shows a schematic illustration of the LB film with vapor-deposited aluminum electrodes and the

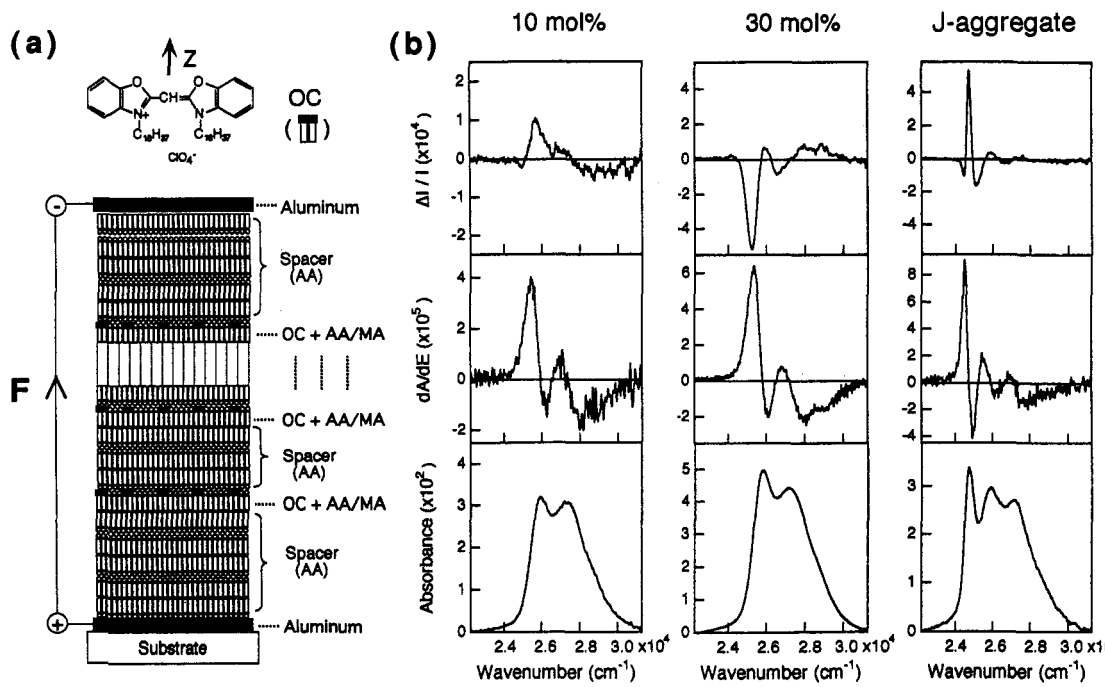

Fig. 3. (a) A schematic illustration of the structure of oxacyanine (OC) LB film with aluminum electrodes; AA, arachidic acid; MA, methylarachidate. (b) Electric-field-induced linear change of ΔI(E)/I(E), the first derivative and the absorption spectra in $S_0 \rightarrow S_1$ of OC. The field strength is 1.1×10^6 V/cm.

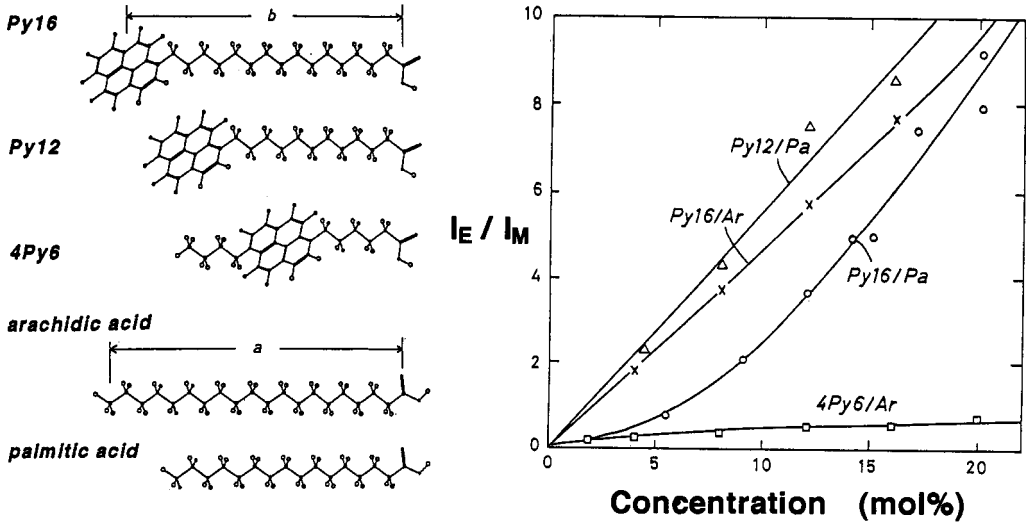

Fig. 4. Plots of the intensity ratio of excimer and monomer fluorescences of pyrene as a function of concentration in LB films of pyrene derivatives with alkyl chains of different lengths.

spectra of $\Delta I / I$, dA/dE and absorbance. It is seen that for 10 mol% and J-aggregate the $\Delta I / I$ spectra are identical with their respective dA/dE spectra, whereas for 30 mol% it is opposite in polarity to the dA/dE spectrum. This means that the aggregate (dimer) is different in nature from the J-aggregate as well as from the monomer: The results are $\Delta\mu_Z = 0.052$ (D), $\Delta\alpha_{ZZ} = 2.5$ ($4\pi\varepsilon_0$Å) for the monomer, $\Delta\mu_Z = 0.19$, $\Delta\alpha_{ZZ} = 2.5$ for J-aggregate, whereas $\Delta\mu_Z = -0.21$ (D), $\Delta\alpha_{ZZ} = 5.1$ ($4\pi\varepsilon_0$Å) for the dimer. It should be noted that the direction of $\Delta\mu_Z$ is opposite to those of the monomer and J-aggregate.

Control of Molecular Dispersion

In LB mixed films with fatty acids, functional guest molecules are gathered with each other owing to their van der Waals forces during the course of formation of a compressed monolayer on water surface. Therefore, one can expect that, if guest molecules have alkyl chains long enough to generate larger intermolecular force with fatty acid, they are dispersed much more uniformly in fatty acid matrix.

We studied the chromophore distribution by monitoring the excimer fluorescence in mixed LB films of pyrene and fatty acid (11). In a series of pyrene derivatives with alkyl chains of different lengths as shown in Fig. 4, the pyrene ring locates outside or inside the membrane. The experimental result (Fig. 4) shows that the excimer formation is suppressed significantly in 4Py6 having alkyl chains in both sides of a pyrene ring. This means that pyrene chromophores are distributed uniformly in a 4Py6-type LB film. This technique is applicable to controlling the spatial distribution of guest molecules in LB films.

PHOTOCHEMICAL PROCESSES IN LB FILMS

Sequential excitation transport in LB multilayers

The photosynthetic light-harvesting antenna in plants is characterized by efficient absorption and transport of photonic excitation energy through a stack of several kinds of chromoproteins to the reaction center. With the LB technique, one can obtain an artificial analogue of biological system, i.e., a stacking molecular architecture in which different kinds of dyes as donors and acceptors are stacked sequentially such that the excitation energy transports in a specific direction through the dipole-dipole interaction.

Figure 5 shows an example of time-resolved fluorescence spectrum demonstrating the sequential excitation energy transport; D, carbazole; A1, oxacyanine; A2, thiacyanine; and A3, indocarbocyanine (12).

Site-selection in the interlayer excitation transfer

In LB monolayer films, dye molecules form different sites of slightly different energy levels. As a consequence of this inhomogeneity, the absorption and fluorescence spectra in general are significantly broad. When the acceptor (A) layer is excited through the interlayer energy transfer from the donor (D) layer, the fluorescence spectrum of A is found to be different in spectral band position from those obtained with direct photoexcitation of A layer. This means that the layer-to-layer excitation transport takes place among specifically selected sites. In a two layer system consisting of a carbazole (D) layer and a oxacyanine (A) layer, as an example, the excitation of carbazole at 295 nm gives a fluorescence spectrum blue-shifted by ca. 10 nm relative to the spectrum from the excitation of oxacyanine at 350 nm (13,14).

Enhancement of the transfer efficiency in the stacking multilayers

In the LB multilayers of D-A1-A2-A3 (Fig. 5), the quantum efficiency of excitation transport Φ_{ET}(D-A1) in D-A1 is enhanced by further stacking A2 layer. Similarly, Φ_{ET}(A1-A2) is enhanced by stacking A3 layer. These phenomena are seen generally in the LB multilayers (14). We propose here a hypothetical

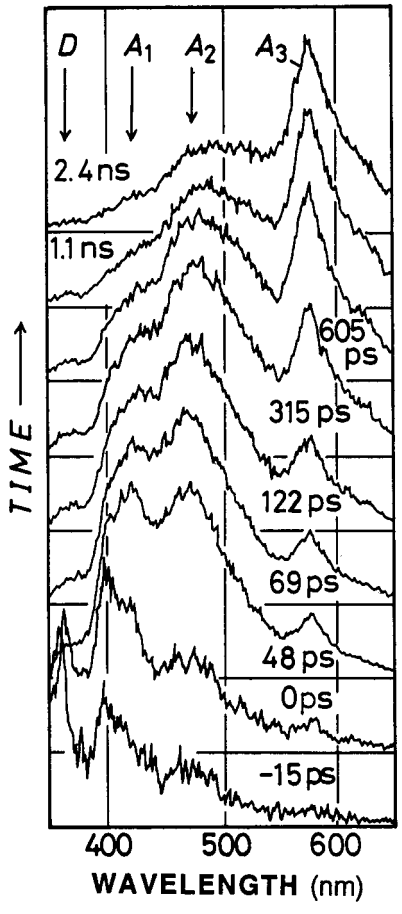

Fig. 5. Time-resolved fluorescence spectra of the LB multilayer film of D-A1-A2-A3. The excitation wavelength is 295 nm.

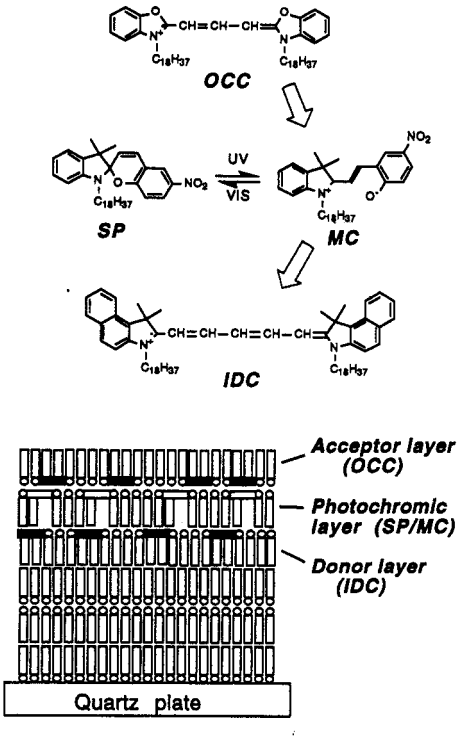

Fig. 6. Structure of the photochromic LB multilayers and the excitation energy transfer pathway. The excitation transport from oxacarbocyanine (OCC) is switched depending on the photochromic reaction between spiropyran (SP) and merocyanine (MC).

mechanism that the Förster-type excitation transfer takes place from highly vibrationally levels of D to the isoenergetic levels of A, i.e., the "hot" excitation transfer occurs competing with the vibrational relaxation within S_1 vibrational manifold of D. The "hot" transfer mechanism is possible only if the A molecule locate nearby D as is the case of LB multilayers, and might be responsible for the site-selection in the interlayer excitation transfer mentioned above.

APPLICATION TO MOLECULAR SWITCHING DEVICES

When the LB multilayer contains dye molecules capable of a reversible photochromic reaction, e.g., spiropyran, the excitation transport can be switched depending on the photochromic reaction between spiropyran (SP) and merocyanine(MC) upon irradiating with UV or visible light (15,16). In this study, the LB multilayers consisting of oxacarbocyanine (OCC), SP and indodicarbocyanine (IDC) were prepared. Figure 6 illustrates a structure of LB multilayers employed here. The energy levels of the lowest singlet states of OCC, MC and IDC are lowered in this order, and the Förster excitation transfer OCC→MC→IDC can take place straightforward in this pathway. On the other hand, the energy level of SP is substantially higher than that of OCC, then the energy transport OCC→SP cannot proceed. Thus the excitation transport is switched depending upon the state of the photochromic molecule, in other words, depending upon irradiation of UV or VIS light.

We can monitor the switching of energy transport by measuring the change of fluorescence intensities of particular layers. The result is shown in Fig. 7. Under UV irradiation (380 nm) where the excitation transport circuit is opened, the excitation is transferred from OCC to IDC and the fluorescence emits from IDC. Under VIS light irradiation (560 nm) where the circuit is closed, the fluorescence emits from OCC. It

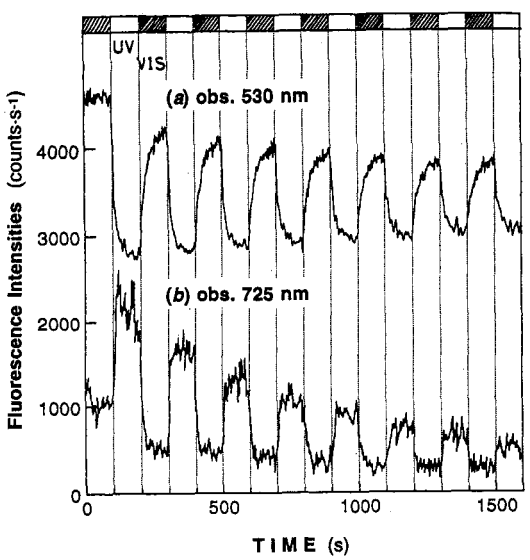

Fig. 7. Fluorescence intensity changes due to an optical switching of the excitation transport.

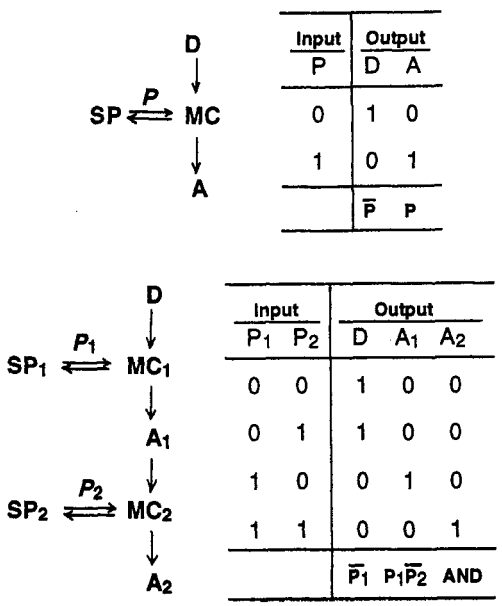

Fig. 8. Schematic diagrams and the truth tables for the excitation transport and its switching by the photochromic reaction.

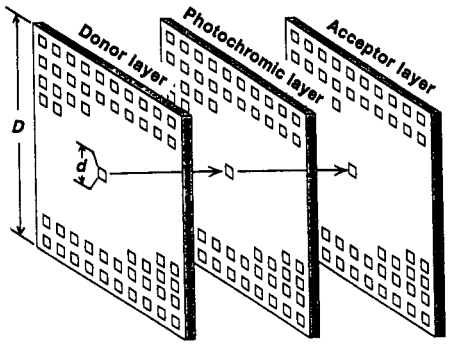

Fig. 9. A model of an optically-switching parallel processor consisting of three monolayers; a donor layer, a photochromic layer and a acceptor layer. D=10 mm, d=1 μm, number of pixels (D^2/d^2) = 10^8.

is seen in Fig. 7 that the fluorescence intensities of OCC and IDC are switched in out-of-phase depending on the irradiation of UV or VIS light.

Applicability to 2D Optical Switching Devices

Let us consider the logics in this optical switching device (17), following a diagram and a truth table shown in Fig. 8. Let the input P=1 and 0 denote UV and VIS irradiation, respectively, and let the output D=1 and 0 mean that the excitation *does* locate and *not* locate at D layer (OCC), respectively. In other words, the 510-nm fluorescence (D) *does* emit in D=1, and *not* emit in D=0. Similarly, the output A=1 and 0 means that the excitation *does* locate and *not* locate at A layer (IDC), respectively, and that the 720-nm fluorescence (A) *does* emit in A=1 and *not* emit in A=0. The relationship between the input P and the output D or A is that for P=0, it gives D=1 and A=0, and for P=1, D=0 and A=1. As a result of this relationship, the output D gives NOT P, while the output A gives P, the same one as the input P.

Now we consider furthermore a photochromic LB device consisting of two serial-connected elements, each of which is the same in structure as shown in Fig. 6, but contain different types of photochromic dyes. The truth table (Fig. 8) shows that as responses to the two input signals P_1 and P_2, the output D gives NOT P_1 similarly to the previous case, the output A_1 gives P_1 × NOT P_2, and the output A_2 gives AND. The molecules for D, SP_1 (MC_1) and A_1 are the same ones as shown above, while the molecules for SP_2 (MC_2) and A_2 are different types of molecules for which we are now testing several candidates.

Since the LB film is a 2D film, the photochromic LB film might be applicable to a pattern logic device or a parallel processor. Let us consider applicability of the present device shown above to a 2D spatial light modulator, following a manner of Tanida and Ichioka (18). Figure 9 shows schematically a structure of the element of parallel processor. We assume here the size of an element (D^2) is 10 mm^2 and the size of a single pixel (d^2) is 1 μm^2. Then the number of pixels included in an element (N^2) is written as $N^2 = D^2 / \alpha^2 d^2 = 10^8$. A factor of α, a margin factor, is introduced in the denominator for avoiding crosstalk. For the moment, α is taken as unity for simplicity of discussion. The total performance of this switching device (P) is expressed as, $P = \nu N^2$, where ν is the switching rate, i.e., a number of repetitive switching (NOT operation as an example) per second. Note that the number of photochromic molecules included in a pixel of 1 μm^2 is 5 x 10^5 molecules in a LB monolayer film of 10 mol% concentration. We take a switching threshold as one half of molecules in a pixel converting to MC. The concentration of a photochemical reaction product is expressed approximately as $[M] = I_0 \times (1 - 10^{-A}) \times \Phi_1 \times t$, where I_0 is the controlling light intensity, $(1 - 10^{-A})$ is the absorptivity, Φ_1 is the reaction quantum yield, and t is the irradiation time. According to knowledge of $\Phi_1 = 0.44$ (16) and the measured value for the absorbance A, the switching (reaction) time, i.e., the time required for accumulating the photoproduct up to the threshold concentration,

was calculated for various types of light sources. It was found that a cw argon-ion laser (5 W) is applicable for the controlling light source, and the switching time is as fast as 0.1 msec ($\nu = 10^4 s^{-1}$). Then the performance of this device is estimated from $P = \nu N^2$ to be 10^{12} NOT operation s^{-1}. This value is comparable with those of other optical switching devices such as liquid crystal light valve ($P = 7 \times 10^9$ operation s-1), optical bistability devices (7×10^{12}), opto-electronic hybrid device (6×10^{14}), and optical computer (OPALS) (1×10^{19})(18). It is concluded that this type of photochromic LB films can be applied to a 2D spatial light modulator as an element in the optical computer.

The authors acknowledge Professor S. Nagakura, President of Graduate University for Advanced Studies, and Professor H. Masuhara, Osaka University, for their continued encouragement and fruitful discussion to this study. This work was supported by the Ministry of Education, Science and Culture, Yazaki Memorial Science Foundation, Research Foundation for Opto-Science (Hamamatsu) and Nissan Science Foundation.

REFERENCES

1. J. Klafter and J. M. Drake, eds. *Molecular Dynamics in Restricted Geometries*, Wiley Interscience, New York (1989).
2. F. Lenci, F. Ghetti, G. Colombetti, D.-P. Hader and P.-S. Song, eds., *Biophysics of Photoreceptors and Photomovements in Microorganisms*, NATO ASI Series A: Life Sciences Vol. 211, Plenum, New York (1990).
3. H. Kuhn, D. Möbius,and H. Bücher, in *Techniques of Chemistry*, Vol. 1, Part 3B, A. Weissberger and B. W. Rossiter, eds., Wiley, New York (1972) pp. 577-701.
4. N. Ohta, S. Matsunami, S. Okazaki and I. Yamazaki, *Langmuir*, in press (1994).
5. I. Yamazaki, N. Tamai, and T. Yamazaki, *J. Phys. Chem.*, **94**, 516 (1990).
6. N. Tamai, T. Yamazaki and I. Yamazaki, *Can. J. Phys.*, **68**, 1013 (1990).
7. N. Tamai, H. Matsuo, T. Yamazaki and I. Yamazaki, *J. Phys. Chem.*, **96**, 6550 (1992).
8. N. Ichinose, Y. Nishimura and I. Yamazaki, *Chem. Phys. Lett.*, **197**, 364 (1992).
9. N.Ohta, N. Tamai, T. Kuroda, T. Yamazaki, and I. Yamazaki, *Chem. Phys.*, **177**, 591 (1993).
10. N.Ohta, S. Okazaki and I. Yamazaki, *Chem. Phys. Lett.*, in press (1994).
11. K. Sumi, N. Tamai and I. Yamazaki, unpublished.
12. I. Yamazaki, N. Tamai, T. Yamazaki, A. Murakami, M. Mimuro, and Y. Fujita, *J. Phys. Chem.*, **92**, 5035 (1988).
13. N. Ohta, S. Okazaki, S. Yoshinari and I. Yamazaki, *Thin Solid Films*, in press (1994).
14. I. Yamazaki, N. Ohta, S. Yoshinari and T. Yamazaki, in *Microchemistry: Spectroscopy and Chemistry in Small Domains*, H. Masuhara ed., Elsevier, Amsterdam (1994) pp. 431-440.
15. T. Minami, I. Yamazaki, T. Yamazaki, and N. Tamai, in *Proceedings of the MRS International Meeting on Advanced Materials*, Vol. 12, M. Doyama, S. Somiya, R. Chang, and S. Tazuke, eds., MRS, Pittsburgh (1989) pp 267-272.
16. T. Minami, N. Tamai, T. Yamazaki, and I. Yamazaki, *J. Phys. Chem.*, **95**, 3988 (1991).
17. I. Yamazaki, S. Okazaki, T. Minami and N. Ohta, *Appl. Opt.*, in press (1994).
18. J. Tanida and Y. Ichioka, *Appl. Opt.*, **25**, 1565 (1986); *Appl. Opt.*, **27**, 2926 (1988).